End Member and Bayesian mixing models consistently indicate near-surface flowpath dominance in a pristine humid tropical rainforest

Article *in* Hydrological Processes · March 2021

DOI: 10.1002/hyp.14153

CITATIONS
0

READS
220

8 authors, including:

Christian Birkel
University of Costa Rica
162 PUBLICATIONS **2,438** CITATIONS
SEE PROFILE

Clément Duvert
Charles Darwin University
34 PUBLICATIONS **567** CITATIONS
SEE PROFILE

Sebastián Granados-Bolaños
University of Costa Rica
10 PUBLICATIONS **32** CITATIONS
SEE PROFILE

Birkel Christian (Orcid ID: 0000-0002-6792-852X)
Correa Alicia (Orcid ID: 0000-0001-6127-2948)
Sanchez-Murillo Ricardo (Orcid ID: 0000-0001-8721-8093)

End Member and Bayesian mixing models consistently indicate near-surface flowpath dominance in a pristine humid tropical rainforest

Christian Birkel[1,2], Alicia Correa Barahona[1], Clément Duvert[3], Sebastián Granados Bolaños[1], Andres Chavarría Palma[1], Ana Maria Durán Quesada[4], Ricardo Sánchez Murillo[5], Harald Biester[6]

[1]Department of Geography and Water and Global Change Observatory, University of Costa Rica, 2060 San José, Costa Rica.

[2]Northern Rivers Institute, University of Aberdeen, AB24 3UF, Aberdeen, Scotland.

[3]Research Institute for the Environment and Livelihoods, Charles Darwin University, Darwin, Australia.

[4]Department of Physics and Geophysical Research Center, University of Costa Rica, 2060 San José, Costa Rica.

[5]Stable Isotopes Research Group and Water Resources Management Laboratory, National University, Heredia, Costa Rica.

[6]Department of Geochemistry, Technical University of Brunswick, Germany

Corresponding author: Christian.birkel@ucr.ac.cr

This article has been accepted for publication and undergone full peer review but has not been through the copyediting, typesetting, pagination and proofreading process which may lead to differences between this version and the Version of Record. Please cite this article as doi: 10.1002/hyp.14153

Abstract: 325 words

Tables: 4

Figure: 7 (color: 7)

Words: 7865 (excluding, title, abstract, reference list)

Key points:

- Rainforest system dominated by a quick, near-surface runoff generation.
- No evidence for deeper and older groundwater.
- Mixing analysis results of EMMA and MixSIAR were largely consistent.
- Catchment geomorphological differences resulted in distinct hydrochemical signatures.

Abstract

The impacts of forest conversion on runoff generation in the tropics have received much interest, but scientific progress is still hampered by challenging fieldwork conditions and limited knowledge about runoff mechanisms. Here, we assessed the runoff generation, flow paths and water source dynamics of a pristine rainforest catchment in Costa Rica using End Member Mixing Analysis (EMMA) and a Bayesian mixing model (MixSIAR). Geochemical tracer data collected over a four-week field campaign were combined with tritium data used to assess potential deeper groundwater flow pathways to the perennial stream. The streamflow composition was best captured using three end-members, namely throughfall, shallow (5 – 15 cm) and deeper (15 – 50 cm) soil water. We estimated the end-member contributions to the main stream and two tributaries using the two mixing approaches and found good agreement between results

obtained from EMMA and MixSIAR. The system was overwhelmingly dominated by near-surface sources, with little evidence for deeper and older groundwater as tritium-derived baseflow mean transit time was between 2.0 and 4.4 years. The shallow soil flow pathway dominated streamflow contributions in the main stream (median 39 % and 49 % based on EMMA and MixSIAR, respectively), followed by the deeper soil (32 % and 31 %) and throughfall (25 % and 19 %). The two tributaries had even greater shallow soil water contributions relative to the main stream (83 % and 74 % for tributary A and 42 % and 63 % for tributary B). Tributary B had no detectable deep soil water contribution, reflecting the morphology of the hillslope (steeper slopes, shallower soils and lower vegetation density compared to hillslope A). Despite the short sampling campaign and associated uncertainties, this study allowed to thoroughly assess runoff generation mechanisms in a humid tropical catchment. Our results also provide a first comparison of two increasingly used mixing models and suggest that EMMA and MixSIAR yield comparable estimates of water source partitioning in this tropical, volcanic rainforest environment.

Keywords: humid tropics, runoff generation, tracers, Costa Rica, water source contribution, EMMA, MixSIAR.

1. Introduction

Much research has examined the impacts of land use changes on hydrological processes in the tropics (Bonell and Bruijnzeel, 2005; Monfreda et al., 2005; Chaves et al., 2008; Wohl et al., 2012; van Meerveld et al., 2019), but experimental research conducted in undisturbed forested areas is limited (see Zhang et al., 2010 as an exception and a global review by Zimmermann et al., 2012),

particularly in humid tropical forests with a geomorphology of volcanic origin (e.g. Muñoz-Villers and McDonnell, 2012; Solano-Rivera et al., 2019). The natural dynamics of hydrological processes and runoff generation are relatively unknown in humid tropical environments despite some early work that goes back to the late 1970s by Bonell and Gilmour (1978). Furthermore, the tropics are generally characterized by high rainfall rates (Chang and Lau, 1983), which - even under undisturbed vegetation cover - can result in high runoff ratios caused by surface flow, and subsequently high streamflows with substantial material transport (Cassells et al., 1985; Thomas, 1994). In such catchments, the rainfall-runoff dynamics tend to be flashy and variable due to rapid meteorological changes and to heterogeneities in the material properties of soils and bedrock interacting with a dense vegetation. Low hydraulic conductivity of shallow soil layers, as observed for instance in a lowland rainforest catchment in Panamá (Zimmermann et al., 2012), can influence the runoff generation processes with surface flow emerging as a prominent mechanism. However, the literature meta-analysis of Barthold and Woods (2015) showed that most of the analyzed tropical catchments were dominated by sub-surface stormflow and runoff generation.

Studies on runoff generation mechanisms and flow pathways in the tropics, as reviewed by Elsenbeer (2001) and later summarized by Barthold and Woods (2015), typically use hydrometric data to characterize the rainfall-runoff relationships together with infiltration measurements and soil physical characteristics, but also often rely on tracer data. Many studies have included stable isotopes of oxygen-18 and deuterium among other conservative tracers such as electrical conductivity and chloride (Leibundgut et al., 2009 for a general reference), but also increasingly

other solutes and even trace elements (Newbold et al., 1995 for an example from Costa Rica; Bücker et al., 2010; Shanley et al., 2011; Wymore et al., 2017). Stable isotope tracers have mostly been used to assess old and new water contributions to streamflow (Barnes and Bonell, 1996; Scholl et al., 2015) and geochemical tracers to determine geographic and/or source waters from different profiles of litter leachate, soil and groundwater and their respective contributions to streamflow (e.g. Elsenbeer et al., 1995).

Uncertainties of tracer-based hydrograph separation and mixing analyses have often been related to large spatiotemporal variations in the chemical signature of source waters contributing to streamflow. Using multiple tracers can help reduce uncertainties and avoid false conclusions about the hydrological functioning of catchments (e.g. Barthold et al., 2011; Correa et al., 2019). In addition to geochemical tracers, radioactive isotopes (e.g. tritium) can be used to assess deeper and older flowpaths to streams, as illustrated by Genereux et al. (2009) and Solomon et al. (2010) who detected regional groundwater flowing into surface water in a volcanic environment of Costa Rica. While the use of multiple tracers can improve our understanding of runoff generation and groundwater flow pathways to streams, the choice of an appropriate numerical approach to assess source partitions and quantify associated uncertainties is equally critical. The end-member mixing analysis (EMMA; Christophersen et al., 1990) has been widely used for hydrograph separation, with uncertainties typically quantified using Gaussian error propagation (Genereux, 1998) or first-order Taylor series approximation (Correa et al., 2019). But the need for models that can cope with both multiple sources and variability within sources has prompted the development of more complex, probabilistic models (Phillips and Gregg, 2003;

Stock et al., 2018; Beria et al., 2020). Model frameworks such as MixSIAR use Bayesian hierarchical modelling techniques and compositional data transformation to assess the likelihood of source proportions (Stock et al., 2018). An increasing number of studies has used Bayesian theory to assess water sources to streams (e.g. Beria et al., 2020; Birkel et al., 2020; Duvert et al., 2020), but a systematic comparison of the relative performances of the EMMA and Bayesian approaches is still lacking (He et al., 2020).

In an attempt to fill the above identified knowledge gaps, we focused our efforts on a short-term, intense experimental campaign similarly to Riveros-Iregui et al. (2018). We collected high-resolution (roughly 8-hourly) streamwater tracer data in the San Lorencito catchment, a 3.2 km^2 tropical pristine headwater located in the Volcanic Cordillera of Tilarán, Costa Rica. The monitoring included soil, stream, throughfall, rocks, and stream tributary tracer data collection complemented by high temporal hydro-climatic data. Earlier tracer-aided modelling work at the same study site (STARR*tropics*) using stable water isotope tracers by Dehaspe et al. (2018) suggested a surficial system with little resilience to impacts. We now attempt to test this model-based hypothesis and explore when, how and where runoff is generated in humid tropical volcanic environments. For this, we combine experimental tracer data, hydrograph separation techniques, two linear mixing models and baseflow transit time analysis with tritium. Our specific objectives are:

i) Combine high resolution tracer sets and hydro-climatic data in a mixing model framework to assess the dominant flow pathways in a relatively data scarce pristine rainforest catchment.

ii) Compare EMMA with a Bayesian mixing model approach to evaluate the uncertainty in geographical source waters and their respective spatio-temporal contributions to the mixture in streamflow.

2. Study area, data and methods

2.1 The biological reserve Alberto Manuel Brenes (ReBAMB) study catchment

The San Lorencito headwater (3.2 km^2) catchment is located in the Volcanic Cordillera of Tilarán at the continental divide in Costa Rica, Central America (Figure 1) and drains towards the Caribbean Sea. This protected (Biological Reserve) and pristine (no historic logging) pre-montane rainforest catchment is typical of tropical volcanic (1 to 7 Million years old with mainly basaltic and andesitic rocks) regions. The geomorphology is characterized by deeply incised V-form valleys and highly dynamic streams emphasized in Figure 1 with hillslope B exhibiting steeper stream slopes compared to hillslope A (Table 1). The geomorphological difference between both hillslopes is reflected in higher terrain ruggedness according to Riley et al. (1999) and sediment transport indices (Moore and Burch, 1986) for the monitored sub-catchments on hillslope B over A (Table 1). The San Lorencito stream is marked by a geological normal fault with the northern hillslope A sliding under the steeper southern hillslope B. The elevation ranges from 870 m to 1470 m with a mean slope of 22° (Table 1). The main channel of the San Lorencito stream has a length of 3.2 km and a mean river slope of 20.5° (16° for sub-catchment tributary on hillslope A and 22° for sub-catchment tributary B). The main soils in the catchment are porous (average porosity of 84%, soil density average of 0.4 g/cm^{-3}) with high infiltration capacities beyond 100 mm/h and an average saturated hydraulic conductivity (kSAT) of 95 mm/h (standard deviation of

70 mm/h). Soil density increases with depth but is always < 0.85 g/cm^{-3} and the hydraulic conductivity decreases with depth with a minimum measured kSAT of 20 mm/h at 90 cm depth at one soil moisture sensor on hillslope A. The paleo Andisols (loamy sands) and less developed Entisols with a mean depth of 0.7 m developed on top of a weathered and likely deep regolith (deeper soils on hillslope A compared to B). The soil texture in the sub-catchment on hillslope A is on average less coarse (sand 57%, loam 24%, clay 19%) compared to the steeper sub-catchment on hillslope B (sand 69%, loam 17%, clay 13%). The vegetation density seems to be linked to the topography, as suggested by higher leaf area indices (LAI) on the lower slopes of hillslope A (sub-catchment average of 3.2) compared to an average LAI of 1.8 in the sub-catchment on hillslope B (Figure 1).

The catchment is characterized by an annual average rainfall of around 2.8 m/year that ranges from 2 to almost 4 m/year for particular years with a relatively low annual potential evapotranspiration of around 0.5 m/year and a moderate dry season from February to April. The mean annual temperature is slightly below 21°C and the relative humidity is constantly high at close to 100%. More detailed information about the catchment characteristics can be found in Dehaspe et al. (2018) and Solano-Rivera et al. (2019). The catchment and research station are managed by the University of Costa Rica (UCR) for the Costa Rican National Park Conservation Authority (SINAC) and forms part of the Alberto Manuel Brenes Biological Reserve (ReBAMB) with restricted access only for research. The baseline hydro-meteorological measurements are located next to the San Lorencito stream and have been recorded since June 2015 (Figure 1).

Figure 1: The regional context of the San Lorencito study catchment with monitored sub-catchment tributaries located on hillslopes A and B, automatic weather station in the forest used for this measurement campaign (blue circle), soil moisture (blue rectangles) and sampling (black triangles) locations, topography and a satellite-derived leaf area index (LAI) map (Dehaspe et al., 2018). The catchment outlet hydrometric and chemistry monitoring station is shown with the red triangle.

Table 1: Catchment, hydro-meteorological and geomorphologic summary statistics of the San Lorencito catchment and the monitored sub-catchment tributaries on hillslopes A and B.

		Total catchment (Q1)	**Sub-catchment A (north)**	**Sub-catchment B (south)**
Descriptor	**Unit**	**Mean [Range]**	**Mean [Range]**	**Mean [Range]**
Area	km^2	3.2	0.21	0.15
Topography				
Elevation	m.a.s.l.	1133.5 [873.7-1472.4]	1015 [878 – 1153]	1022 [878 – 1148]
Slope	°	22.3 [0.15-52]	16.4 [5-63]	16.8 [9-68]
Drainage Density (1:200000)	km/km^2	0.016	0.0039	0.0046
Stream Slope	°	20.5	16.3	21.8
Sediment Transport Index	-	0.37 [0-39]	0.20 [0 - 6.11]	0.55 [0 - 26.2]
Terrain Ruggedness Index	-	1.63 [0.01-5.03]	1.5 [0.02 - 4.1]	1.8 [0.1 - 4.3]
Hydroclimatic (2015-2018)				
Annual P	mm	2789 [1935-3787]		
Annual PET	mm	490 [332-579]		
Annual Q	mm	2099 [1343-2446]		

2.2 Data collection and analytical methods

An in-situ sensor measured water level (Global Water WL400-015-025) in an accessible and protected section at the outlet of the San Lorencito catchment (Figure 1). The sensor was installed and routinely cleaned and checked for drift. Data were stored every 5 minutes using a Global Water GL-500 logger (precision of ±5 mm). Meteorological data (throughfall, temperature, humidity, radiation, pressure, wind direction and speed) were measured using a HOBO station

located within the forest (890 m a.s.l) at a distance of 50 m from the stream (weather station in Figure 1). We previously assessed the spatial variability of meteorological inputs along a 400 m elevation gradient of the catchment and found relatively limited variations (Dehaspe et al., 2018; Solano-Rivera et al., 2019). Throughout the entire monitoring period, manual discharge gaugings (salt dilution and current meter) of the main stream at the outlet and of the two tributaries were performed weekly and on an occasional event-basis. The gaugings taken at the outlet were used for the construction of a rating curve that converts measured water level into discharge (Solano-Rivera et al., 2019). The rating curve for the main stream was adjusted to match the annual water balance. Soil moisture was measured at 15 min intervals with Odyssey multi-profile sondes configured to register at 10 cm, 30 cm, 50 cm, 70 cm and 90 cm depths and a resolution of ±0.01 %. Sondes were installed along two opposite hillslope transects of the sub-catchments on hillslopes A (3 sondes) and B (2 sondes) and calibrated with in-situ soil physical measurements of texture and saturated hydraulic conductivity per depth increment (Figure 1).

Streamwater samples for tritium analysis were collected at progressively lower flows in February, March and April 2018 (streamflow at the outlet decreased from around 100 L/s in February to a minimum of 45 L/s in April showing an increase in electrical conductivity from 30 µS/cm to 80 µS/cm) and analyzed at the Australian Nuclear Science and Technology Organisation (ANSTO) in Sydney. Event and monthly rainfall samples (500 to 1 L) were collected for tritium analysis from 2015 to 2017 at the Universidad Nacional, (UNA) in Heredia, stored in a fridge immediately and sent for analysis to the International Atomic and Energy Agency (IAEA) isotope laboratory in Austria, Vienna. Streamflow and rainfall samples were distilled and electrolytically enriched

(between 67- and 70-fold) prior to counting with a liquid scintillation counter for several weeks. The limit of quantification was 0.07 tritium units (TU) for all samples, and analytical precision was between ±0.03 and ±0.06 TU for streamflow and between ±0.05 and ±0.18 TU for rainfall.

Streamwater samples were collected manually for trace element analysis (14 samples) in the San Lorencito main stream at the outlet over a four-week period from 24th May to 18th June 2017, right after the start of the rainy season in April. Manual sampling in the main stream was complemented with an automatic ISCO 3700 water sampler programmed to retrieve samples over an eight-hour cycle (28 samples used for analysis). Additionally to the main stream sampling, we also manually monitored two hillslope tributaries (A and B; Figure 1). At the northern sub-catchment tributary A, we manually collected 10 samples and at the southern sub-catchment tributary B, we collected 12 samples simultaneously with the main stream. Unfortunately, it was only possible to collect a single composite throughfall sample over two weeks from 25th May to 7th June using a PALMEX device (Gröning, 2012) at the weather station location in the forest. We also milled the dominant bedrock (three replicate Andesites and pyroclastic lava flow samples) and prepared a solution with distilled water for analysis after continuously stirring at average stream temperature of 20°C for 24 hours, assuming this would represent natural conditions of waters in contact with weathered rock.

Soil samples for trace element analysis were collected at three soil profiles covering the elevation gradient at both sub-catchments of hillslopes A and B in the first week of June 2017 (Figure 1). Three depth-averaged samples at each hillslope were taken at 10 cm and 40 cm corresponding

to the organic *Ah* horizon and a mineral *Bv* horizon of the volcanic Andisol or Cambisol soils. Solid samples (0.5 kg) were stored in Whirl Packs and refrigerated at 4°C until analysis. In the laboratory, three replicate solid soil samples (10 g of fresh homogenized soil material) were mixed with 100 mL water (1:10 ratio) and shaken for 24 hours. Then, the suspension was vacuum-filtered (0.45 µm) and the leachates stabilized with 60% pure nitric acid for element analysis (35 solutes) with an Inductively Coupled Plasma Mass Spectrometer (ICP-MS; Agilent 7700, Germany) in the geochemical laboratory at the Technical University of Brunswick, Germany. The quality of the measurements was controlled by a river water reference material (LGC6019) with known concentrations for the solutes used. Deviation of measured concentrations from the reference was always < 1.6% and always within the given standard deviation (Balzer et al., 2020). The latter analytical method was applied to all liquid, soil and stream samples.

2.3 Tracer-based mixing, hydrograph separation and transit time models

***Baseflow digital filter*:**

A simple baseflow separation was conducted using the one-parameter recursive digital filter according to Arnold and Allen (1999). The filter parameter α was hereby fixed at 0.925 as proposed by Nathan and McMahon (1990):

$$Qs(t) = \alpha Qs(t-1) + \frac{1+\alpha}{2}\big(Q(t) - Q(t-1)\big) \qquad \text{Eq. 1}$$

The baseflow fraction *Qb* is derived from total streamflow *Q* minus surface or quickflow *Qs*. The calculated digital filter baseflow was then compared to two tracer-based, linear mixing approaches, (1) the traditional EMMA and (2) a model based on Bayesian theory (MixSIAR).

***End Member Mixing Analysis (EMMA) and selection of tracers*:**

We used End Member Mixing Analysis (EMMA) (Hooper, 2003) for the identification of geographical water sources and their contribution to the river. This methodology assumes that a stream is a mixture of geochemical signatures of sources (Christophersen et al., 1990) following a linear mixing process (Hooper, 2001). The river observations should ideally be bounded by the selected sources, however, when the observations fall outside the mixing diagram of the water sources these are projected onto the domain in order to avoid negative contributions (Liu et al., 2004). The latter can occur due to input-data uncertainty or time and space-dependent end-member variability (Chaves et al., 2008). A key point for the reliable use of EMMA is that tracers should be conservative and not be involved in adsorption or biological processes (Hooper, 2001). From a suite of elements almost spanning the periodic table, we assumed that the tracers Ca, K, Fe, Mg and Na behave conservatively based on tracer versus tracer bivariate scatter plots from stream data (Barthold et al., 2011; James and Roulet, 2006) with negligible co-linearity (selection criterion: R^2 value >0.5; p-value <0.01). The co-linearity analysis followed a principal component analysis (PCA) and residual error plots to assess the dimensionality of the hydrological system according to Hooper (2003). Mg and Na were excluded from our analysis because these tracers were not available for the bedrock end-members. The lowest residuals between the projected and original stream tracer values with a random distribution defined the system dimensionality

(Hooper, 2003; James and Roulet, 2006) (see Figure 2). The source end-members were projected into a PCA-space generated from stream samples and used to calculate water source contributions to the stream. For a detailed description of the methodology, readers are referred to Christophersen et al. (1990). Uncertainties in source contributions were calculated based on first-order Taylor series approximation (Phillips and Gregg, 2001; Correa et al., 2019). The water source proportions in streamflow were estimated over the four-weeks monitoring campaign overall, and for each event separately using the selected conservative tracers Fe, Ca and K. The source end-members considered were (i) throughfall, (ii) shallow soils at 10 cm, (iii) deeper soils at 40 cm depths and (iv) bedrock. The same source contributions were tested for both monitored sub-catchment tributaries on hillslopes A and B. Our assumptions related to the source end-members were, firstly, that the two-weeks composite throughfall sample is representative of the complete four-weeks study period (time-invariance) and of the catchment (space-invariance). Secondly, the soil end-members are assumed time-invariant over the study period.

Figure 2: Bi-variate plots (upper row) of conservative tracers and resulting unstructured residual error plots of Fe, Ca and K stream chemical parameters (lower row) aiding selection of conservative tracers without structure in the residuals.

***Bayesian mixing model (MixSIAR)*:**

As a second tracer-based approach to hydrograph separation, we used the *R* package MixSIAR (Stock and Semmens 2016; Stock *et al.* 2018), which implements linear mixing equations in a Bayesian framework. We chose MixSIAR because it has the ability to incorporate source

variability and to provide robust assessments of the likelihood of source proportions through a Markov chain Monte Carlo (MCMC) algorithm. As with EMMA, we applied the model to our data to determine the relative contributions of each water source to the main stream and tributaries. The water source proportions were estimated over the four-weeks monitoring campaign, and for each event separately. We considered the same assumptions of time-invariance and representativeness of the three sources i.e. throughfall, shallow soil, deeper soil and bedrock, and used the three tracers previously identified as conservative tracers (Fe, Ca and K). We used generalist priors (α set to 1 for each source) and ran 100,000 iterations of the MCMC loop (burn-in 50,000), which allowed us to obtain 3,000 posterior density estimates for each source contribution. In the results, we report the median and distribution (interquartile range and 5^{th}-95^{th} percentiles) from these 3,000 estimates.

***Baseflow mean transit time model*:**

In addition to the short-term, high-resolution measurement campaign in 2017, we assessed potential deeper flow pathways by estimating water transit time under low baseflow conditions. The baseflow transit time is assumed to reflect the mean age of groundwater contributing to the stream. Transit time was obtained using three streamwater tritium (^{3}H) samples collected at progressively lower flows during the dry season from February to April 2018. In absence of measured long-term tritium data in rainfall in Central America, we reconstructed an input function for the transit time model derived from monthly ^{3}H measurements in rainfall from the nearest northern Hemisphere stations at Menlo Park, California, Miami, Florida and Ocala, Florida (IAEA-GNIP database, 2019). This averaged input function was forced to match ^{3}H

measurements in rainfall from Costa Rica for the years 2015 to 2017. We used monthly precipitation volumes from the NCEP global rainfall product (Willmott and Matsuura, 2001) from 1949 pre-bomb peak until December 2018, which was previously found to match observed rainfall over Central America (Muñoz-Jiménez et al., 2018). The time-invariant transit time distribution function (g) was driven by this input function (C_{in}) and adjusted to match our streamflow ^{3}H measurements (C_{out}), using a convolution integral (Małoszewski and Zuber 1982):

$$C_{out}(t) = \frac{\int_0^\infty C\ \ (t-t_e)P(t-t_e)e^{-\lambda t_e}g(t_e)dt_e}{\int_0^\infty P(t-t_e)g(t_e)dt_e} \qquad \text{Eq. 2}$$

where t_e is time of entry in the catchment, $e^{-\lambda te}$ is a decay term that accounts for ^{3}H decay once in the ground (λ = 1.54x10^{-4} days^{-1}), and P is monthly precipitation. We used a versatile two-parameter Gamma model as transit time distribution function (g). The range of best-fit Gamma model parameters α (dimensionless shape) and β (scale in months) were identified using 100,000 Monte Carlo simulations in the range [0 – 3] for α and [1 – 5000] for β. Each simulation was evaluated using the mean absolute error (MAE) between the model outputs and measured C_{out} values. We kept the absolute minimum MAE simulation for visualization and the 10 % lowest MAE simulations assessing the range of possible baseflow ages. All analyses were performed using the *R* statistical language (R development team, 2019).

3. Results

3.1 Rainfall-runoff response

We selected the five highest magnitude rainfall-runoff events out of ten runoff responses to rainfall input over a four-week monitoring campaign in May/June 2017 (Figure 3; Table 3). Event 2 exhibited the highest throughfall magnitude of 61 mm over 6 hours with a maximum intensity of over 30 mm/h resulting in a peak discharge of 3.8 m^3/s, followed by Event 1 (34.4 mm), Event 5 (17.8 mm) and Event 3 (15.6 mm) (Table 3). The streamflow response of event 2 had an estimated return period of three months based on the total 3.5 years streamflow record. The streamflow response to throughfall inputs was relatively quick with a lag time of around 30 min, in line with Solano-Rivera et al. (2019). Minimum streamflow was at around 120 L/s right before the first event and receded back to 125 L/s at the end of the campaign. Soil moisture showed a rapid response to throughfall inputs at both averaged 10 cm and 50 cm depths resembling the streamflow dynamics (Figure 3b). The deeper soil moisture dynamics at 50 cm were dampened compared to the dynamics at 10 cm depth (Figure 3b). Generally, the sub-catchment on the northern hillslope A retained slightly more soil moisture compared to B and sub-catchment A demonstrated a threshold-effect with sudden increase in soil moisture content at 50 cm after a certain rainfall volume entered the system during event 2. According to the applied digital baseflow filter results, the baseflow contribution sharply decreased at peak flow to close to zero, indicating a large dominance of potential surface runoff during events (Figure 3c).

3.2 Tracer concentrations in streamflow and end-members

The measured concentrations of all sampled water (throughfall, mainstream, tributaries, soils and rocks) are given in Table 2. The Fe concentrations increased in streamflow during runoff events, particularly for events 1 and 2, from slightly below 1 µg/L to a maximum of above 5 µg/L

during event 2 (mean = 1.44 µg/L). In contrast, K (minimum of 0.6 mg/L on various occasions with an average of 0.8 mg/L) and Ca (minimum of 1.8 mg/L during event 2 with an average of 2.3 mg/L) decreased with increasing flow (Figure 3d, Table 2). Sub-catchment tributary A showed lower average Fe concentrations (1.37 mg/L) compared to the mainstream and tributary B had higher average concentrations (1.6 mg/L). A similar trend was observed for K concentrations (0.75 mg/L at tributary A and 1.2 mg/L at tributary B), whereas tributary A showed higher Ca concentrations (4 mg/L) and tributary B lower Ca concentrations (0.34 mg/L) compared to the main stream. The soil samples had higher Fe concentrations, but lower Ca and K concentrations compared to the stream and tributaries, and in throughfall we observed higher Fe and K concentrations compared to the stream and tributaries (Table 2). The large differences in concentrations between different water sources enabled the following mixing model analysis.

Figure 3: Time series plots of the four-weeks sampling period from 24th May to 18th June 2017 showing a) 30 min throughfall, air temperature, b) averaged soil moisture at 10 cm and 50 cm depth for each sub-catchment on hillslope A and B and c) streamflow at the outlet with a digital filter derived baseflow fraction. The last panel d) shows the three selected tracer (Ca, K, Fe) concentration time series in streamflow at the outlet.

Table 2: Summary statistics (mean [standard deviation]) of selected conservative tracers in all potential sources (averaged shallow and deeper soil leachates A and B and 2-week composite throughfall) and the mixture (main stream Q1, tributaries A and B).

	Fe (µg/L)	**Ca (µg/L)**	**K (µg/L)**	**n***
SOURCES				

Throughfall	1.8	1330	2030	1
Soils A (right)	6.03 [12.6]	1500 [1650]	340 [420]	11
Soils B (right)	5.8 [9.8]	1610 [1570]	3 [400]	13
Andesite	205	166400	6240	1
Pyroclastic lava flow	141	22420	2793	1
MIXTURES				
Main stream Q1	1.44 [2.36]	2257.5 [146]	802.4 [63.8]	42
Tributary A (right)	1.37 [0.97]	3990 [0.17]	750 [75]	10
Tributary B (left)	1.6 [0.92]	3430 [280]	1150 [140]	12

*n represents the number of samples

3.3 Estimating water source contributions to mixtures with EMMA and MixSIAR

The EMMA mixing diagram shows the source waters in relation to streamflow and to sub-catchment tributaries A and B (Figure 4). Outlet streamflow samples plotted within the mixing triangle of throughfall, shallow and deeper soil water samples, with only a few samples falling outside the triangle. The EMMA analysis was based on the median and standard deviation of measured concentrations in water sources (Table 2) and individual stream mixtures. The two principal components captured 84% of the total observed variance. Our data for the tributaries plotted slightly outside the EMMA space, with sub-catchment tributary A scattered closer to the shallow soil water samples and the sub-catchment tributary B scattered between throughfall and shallow soil. The potential source component of bedrock (Table 2) as an indicator for groundwater contact time was discarded due to the higher concentrations (several orders of magnitude) in these samples compared to streamwater and tributaries. The source component of rocks plotted therefore far outside the mixing diagram. Although mathematically possible, the bias introduced in the resulting mixing diagram did result in infinitesimal and physically unreasonable small contributions to the mixture of this “geological end-member”.

Figure 4: EMMA mixing diagram using ordered Eigenvectors and source water contributions (throughfall, shallow and deep soils) to the main stream and both sub-catchment tributaries A and B, explaining 84% of the total variance. The error bars represent the first standard deviation of measured concentrations. The single composite throughfall sample was assigned a standard deviation of one.

Spatial variability of source water contributions:

The two mixing models EMMA and MixSIAR generally showed comparable results, particularly for the median source water contributions (Figure 5). The shallow soil flow pathway dominated streamflow contributions in the main stream (median 39% and 49% based on EMMA and MixSIAR, respectively), followed by the deeper soil (32% and 31%) and throughfall (25% and 19%). The steeper tributary B did not exhibit a detectable deeper soil component according to EMMA, and below 10% with the Bayesian model. The shallow soil water together with throughfall were the most important contributing sources to tributary B according to EMMA, while MixSIAR identified the shallow soil water as the sole most important source to tributary B (Figure 5). Both methods agreed on the shallow soil water as the most important source contribution (end-member) to the less steep and with deeper, more developed soils sub-catchment tributary A, which consisted of around 80% shallow soil, 10% throughfall and some minor deeper soil contribution (<10%). The EMMA model performed less well for the tributaries (throughfall for tributary B and shallow soil for tributary A are mathematically beyond the physically possible 0-100 % range) due to the high number of tributary samples falling outside the mixing diagram, whereas MixSIAR properly dealt with this issue as it yielded lower uncertainties for tributaries.

Figure 5: The EMMA (upper panel) and MixSIAR (lower panel) derived source water contributions to the main stream at the outlet, sub-catchment tributary A and B. The boxplots represent the distribution of potential source water contributions derived by a Bayesian approach for MixSIAR and a Taylor series approximation for EMMA. Throughfall (light blue), shallow (brown) and deep (yellow) soil source waters are similarly color coded throughout the paper. The boxes show the median and $25^{th}/75^{th}$ percentiles with the whiskers indicating the $5^{th}/95^{th}$ percentiles. The crosses point out absolute extreme values.

Temporal variability of source water contributions:

The time-invariant throughfall and soil water sources were interpolated to estimate event source water contributions using EMMA and MixSIAR. Both methods showed a relatively good agreement overall (Figure 6) with the exception of the first two streamflow events. For events 1 and 2, MixSIAR estimated a larger deep soil water contribution (close to 50%) compared to EMMA (only about 20-25%). Despite comparable overall median percent contributions, EMMA showed a decreasing trend for shallow soil contributions with decreasing event magnitude (events 3, 4 and 5 in Figure 6), while the Bayesian model estimated a relatively constant shallow soil source for events 3, 4 and 5. Both methods suggested that shallow soil was the most important flow pathway across streamflow events of different magnitude. If shallow and deeper soil sources were combined to form the baseflow component of streamflow (Table 3), both mixing models predicted, on average, 80% of baseflow for the five events occurring during the four-week period. The EMMA model resulted in a higher temporal baseflow variability compared

to MixSIAR as evidenced by a higher standard deviation calculated for the five events (13% compared to 2%, respectively). In contrast, the baseflow digital filter resulted in 35% average baseflow with 30% standard deviation (Table 3) due to an overwhelming quick flow contribution to the larger storm events.

Figure 6: a) EMMA and b) MixSIAR interpolated hydrograph separation time series and source water contributions for each of the five events separately assuming time-invariant end-members (same color code as in previous plots).

Table 3: Rainfall-runoff event characteristics of the sampling period in terms of magnitude (Ptotal), duration, maximum intensity (Imax), time lag between peak throughfall and runoff (P_Qlag), average event baseflow fraction using a digital filter (Qbf@Qp), using EMMA (Qbe@Qp) and MixSIAR (Qbm@Qp) with the latter two methods accounting for baseflow as the sum of shallow soil plus deeper soil water contributions.

Event	**Ptotal (mm)**	**Duration (h)**	**Imax (mm/h)**	**Qp (m^3/s)**	**P_Q lag (h)**	**Qbf@ Qp (-)**	**Qbe@Qp (-)**	**Qbm@Qp (-)**
1) 27/05	34.4	2.5	27	1.2	0.5	0.09	0.94	0.81
2) 28/05	61.8	6.5	34.6	3.83	0.5	0.06	0.82	0.85
3) 02/06	15.6	5	5.6	0.72	0.5	0.25	0.87	0.83
4) 05/06	10	1	10	0.45	0.5	0.67	0.78	0.81
5) 10/06	17.8	4	8.4	0.41	1	0.66	0.59	0.82
AVG	***27.92***	***3.80***	***17.12***	***1.32***	***0.60***	***0.35***	***0.80***	***0.82***
STD	***21.01***	***2.14***	***12.87***	***1.44***	***0.22***	***0.30***	***0.13***	***0.02***

Table 4 gives the generally comparable uncertainties for both mixing models and the three water sources using the median and the 25^{th}/75^{th} percentiles corresponding to the boxes in Figures 5 and 6.

Table 4: Uncertainty ranges of event source water contributions (%) for deeper soils, shallow soils and throughfall determined for EMMA and MixSIAR (sources are ordered identical to Figure 6 from deeper, shallow soil to throughfall).

		Event 1			Event 2			Event 3			Event 4			Event 5		
	Source	Median	Q_{25}	Q_{75}	Median	Q_{25}	Q_{75}	Median	Q_{25}	Q_{75}	Median	Q_{25}	Q_{75}	Median	Q_{25}	Q_{75}
EMMA	Deep soil	22.4	18.4	28.5	32.1	21.2	33.7	27.9	23.1	29.0	31.7	31.6	31.7	37.7	33.0	42.5
	Shallow soil	72.4	62.9	77.2	49.1	46.2	57.5	57.1	54.0	68.0	46.4	40.7	52.1	31.3	25.0	38.6
	Throughfall	5.7	2.9	9.7	17.7	15.0	20.7	15.0	8.6	17.1	22.0	16.3	27.8	31.3	20.4	33.2
MixSIAR	Deep soil	43.2	38.9	52.3	43.9	36.7	68.6	35.3	31.6	48.2	32.4	30.7	34.1	34.6	31.5	37.9
	Shallow soil	38.6	30.0	44.6	39.8	21.6	44.8	46.5	37.6	49.4	48.9	48.6	49.2	49.8	48.5	50.8
	Throughfall	18.4	15.8	21.2	15.9	9.8	19.1	18.5	14.5	19.3	18.6	17.3	20.0	15.3	13.7	18.9

3.4 Tritium-derived baseflow mean transit time as deeper flowpath indicator

The potential for a deeper and older groundwater contribution to baseflow was assessed with tritium age dating. Tritium activity in the stream decreased with decreasing flow (from 0.99 TU in February to 0.78 TU in April with analytical errors of around 0.05 TU), suggesting that the baseflow contribution became progressively older. However, because these streamflow values were largely comparable to our most recent tritium measurements in rainfall in Costa Rica (in the range of 0.7 to 1.5 TU), baseflow was unlikely to originate from deep groundwater sources older than 60 years (approximate detection limit of tritium). This assumption is confirmed by our mean transit time (MTT) modelling: we found that the baseflow MTT ranged from 2 to 4.4 years, with a best-fit MTT of 2.7 years (Figure 7). The best-fit gamma model parameters were *alpha* = 1.3 (-) and *beta* = 25 months. Such a shorter baseflow MTT only supported a surficial flow path dominated system, with little older water derived from deeper storage below 50cm soil depth contributing to sustain baseflow over prolonged dry periods.

Figure 7: The best-fit tritium-based mean transit time (MTT) estimate of baseflow in the San Lorencito stream (Qsim_TU) using reconstructed long-term monthly precipitation volumes (NCEP re-analysis product) and tritium measurements from nearby IAEA stations (Florida and California) merged with recent rainfall measurements in Costa Rica (P_TU) fitted to match the observed tritium in streamflow at the outlet (Qobs_TU).

4. Discussion

4.1 Dominant flowpaths and runoff generation in tropical rainforest catchments

The ongoing debate about the dominant flow pathways generating streamflow in the humid tropics dates back to the 1970s. Bonell and Gilmour (1978) showed for their Babinda catchments in eastern Australia, using various methods including tracer approaches, that Hurricane-induced extreme rainfall generated surface flow via both infiltration excess (Horton) and saturation excess overland flow. Saturation excess overland flow was also observed in Panamanian lowland rainforests due to low soil hydraulic saturated conductivities, high soil density and low permeability below 20 cm depth (Godsey et al., 2004; Zimmermann et al., 2012). Despite a similar rainfall regime, the San Lorencito catchment is of an exclusively volcanic origin resulting in more permeable Andisols as opposed to the sedimentary siltstone geology and older finer grained and much less permeable Ferric Cambisols in these Panamanian catchments. The importance of saturated hydraulic conductivity was emphasized by Johnson et al. (2006) who showed that the permeability of shallow soil layers plays a major role in regulating runoff generation processes in Amazonian headwater catchments. In a land use change context, Ziegler et al. (2008) and Chaves

et al. (2008) also observed overland stormflow in a Thai and a Brazilian catchment, respectively, with a clear increase of surface runoff generation after forest clearance compared to pasture and forest. Recently, van Meerveld et al. (2019) reported a slowing of surface runoff generation with forest recovery in a Philippine catchment. Similar to our results, lateral sub-surface runoff generation and zero surface flow were observed in tropical rainforest catchments on more permeable volcanic substrates such as in Mexico (Muñoz-Villers and McDonnell, 2012) and Puerto Rico (Scholl et al., 2015).

Our steep, volcanic study site on permeable Andisols in northeastern Costa Rica fell in the above category of dominant sub-surface flow pathways, albeit slightly shallower compared to Muñoz-Villers and McDonnell (2012) (on average 44% of shallow soil water and 22% throughfall contributions to the main stream), which according to the meta-analysis of Barthold and Woods (2015) prevails in the tropics. Even though rainfall intensities (>40 mm/h) can be extreme in San Lorencito, the measured infiltration capacities (>100 mm/h) always exceed the physically probable maximum rainfall intensity, and Horton infiltration excess overland flow can be safely excluded as a likely surface runoff generation mechanism. Nonetheless, Solano-Rivera et al. (2019) identified a hillslope-stream connectivity in the most extreme rainfall events as evidenced by soil erosion and transport of materials to the stream, which indicates that some version of saturated conditions and overland flow may occur. The most obvious mechanism of such a surface flow path is saturation excess runoff. The mixing model results presented here do not directly support a saturation excess runoff generation mechanism and we preferred to refer to dominant near-surface flow pathways similar to Tetzlaff et al. (2014). Generally, the soil physical

characteristics play a crucial role in determining the dominant runoff generation mechanisms and flow pathways even under undisturbed forest cover and independent of terrain slope in the tropics, as recently pointed out by Wymore et al. (2017), reviewed earlier by Elsenbeer (2001) and critically appraised by Bruijnzeel (2004). Our spatial comparison between the sub-catchment tributaries A and B supports the soil control on near-surface runoff generation in pristine rainforests, which according to Zimmerman et al. (2012) is likely a much more widespread phenomenon than previously thought (Sidle et al., 2006). We found a quicker and shallower near-surface runoff generation in the steeper and more coarse-grained soils of the southern sub-catchment tributary B, without indication of much deeper soil end-member contribution, as opposed to the less steep northern tributary A with a more significant deeper soil end-member contribution to streamflow.

Despite the importance of the critical zone to modulate runoff generation and a widespread focus on the stormflow-producing mechanisms and flow pathways in the tropics, it is the deeper groundwater contributions to streamflow that sustain low flows over prolonged dry periods (Bruijnzeel, 2004). Usually, different tracers are needed to assess such deeper and likely older water contributions to streamflow. Stable water isotopes allow estimates of water ages up to around 4 years and derived transit time distributions (TTD) are usually less well constrained for the older water contributions characterized by the distribution's tail (e.g. Stewart et al., 2010; Birkel et al., 2016). Correa et al. (2020) estimated a mean catchment transit time of less than 6 months using a tracer-aided rainfall-runoff model in the San Lorencito catchment, indicating a dominance of younger water that is quickly supplied to the stream. Genereux et al. (2009) and

Solomon et al. (2010) used helium, radiocarbon and chlorine age dating tracers to identify and quantify a deeper and old groundwater contribution to a Caribbean lowland catchment at La Selva, Costa Rica originating from a regional groundwater flow recharged into very young (Pleistocene) volcanic rock. Similarly, we used a few tritium low flow measurements at San Lorencito to gain understanding of the range of baseflow ages. We did not find evidence for old groundwater at low flows. Despite being a perennial stream with a mean discharge of around 0.3 m^3/s, the San Lorencito discharge decreases significantly over a few weeks of low rainfall to less than 50 L/s (absolute observed minimum 20 L/s in April 2016). This is in contrast to tropical Andean catchments that maintain a high low flow volume at the end of the dry season due to significant groundwater storage and lateral connectivity (Clark et al., 2014). The tritium analysis was applied as a complementary tracer to generate a more complete picture of the suite of flow pathways and runoff components composing streamflow at high, medium and low flows in line with Farrick and Branfireun (2015). Again, the combination of different tracers with hydrometric approaches and tracer-aided modelling (Dehaspe et al., 2018; Correa et al., 2020) showed that runoff generation and flow pathways composing the San Lorencito streamflow originates in the first 50 cm of soil, with the bulk of water being generated in the first 15 cm of soil (shallow layer).

4.2 Comparison of two widely used mixing approaches

The EMMA approach has been used in hydrology for almost three decades since Christopherson et al. (1990). Bayesian approaches of mixing models have been developed more recently with a strong focus on ecology and stable isotopes (Parnell et al., 2013), and they are now increasingly applied to ecohydrology research (Rothfuss and Javaux, 2017). More widespread use of Bayesian

approaches also promoted recent applications of Bayesian mixing models in catchment hydrology research (e.g. Beria et al., 2020; Duvert et al., 2020). Bayesian mixing models were mainly developed to account for the uncertainty of multiple sources that contribute to a mixture, e.g. in plant water use (Walker and Richardson, 1991), that cannot be resolved with analytical solutions to simple mass balance equations. Therefore, efforts to include uncertainty estimations into mixing models dates back to the early 2000s (Phillips and Gregg, 2001; Soulsby et al., 2003) with recent developments by Correa et al. (2019) using Taylor series approximation for multiple sources (also used here for comparison). The uncertainty often arises due to the input data and temporal and spatial variability of end-members (e.g. James and Roulet, 2006) and the mathematical challenge of resolving chemically similar sources contributing to a mixture (Davis et al., 2015). Here, we faced the challenge of a single available two-weeks composite throughfall sample and a single soil sampling campaign, which led to the assumption of time-invariant source end-members. Despite the uncertainty introduced due to the assumption of time and space-invariance, the composite throughfall sample captured four out of five events analyzed and integrated the complete spectrum of rainfall intensity, duration and magnitude (Figure 3 and Table 3). We, therefore, expected this composite sample to closely represent the average chemical composition of each throughfall event over the measurement period, as supported by a seasonal temporal persistence of throughfall solute concentrations found in other tropical forests (Zimmermann et al., 2007 and 2008). We also based this assumption on the stable isotope composition of the sample (not reported) that resembled the average seasonal value of generally much more variable isotopic throughfall composition compared to solute concentrations. However, we recognize that a single composite sample is not able to capture the spatial

variability of throughfall in tropical forests (Loescher et al., 2002; Holwerda et al., 2006). We still used this sample due to the different solute concentrations particularly for Fe and K compared to the soil concentrations (Table 2). Furthermore, we assumed wide, un-informative priors for the uncertainty analysis of end-members attempting to account for this shortcoming in sampling. The resulting impact on the source contributions to a mixture would therefore be limited to the reported posterior uncertainty (Table 4). Even with the throughfall end-member shifting beyond the established concentration ranges, the explored source contributions would likely enhance the shallow soil end-member dominance and further support our conclusion on quick, near-surface flow pathways. Similarly, we are aware of the potential uncertainty of time-invariant soil end-members, but we assumed that the iron-accumulating soils (Balzer et al., 2020) show a relatively slow reaction to soil moisture variability and constantly high soil moisture over our four-weeks measurement campaign. We, therefore, substituted time with space and incorporated the spatially-distributed soil chemical characteristics into the explicit uncertainty assessment of both mixing analysis methods. Recognizing the spatial variability of geomorphic origin in our study catchment, we investigated two tributaries and their streamwater composition with large geochemical differences related to topography, soil depth and texture and vegetation density (Figure 5). Similarly, streamwater composition varied over time according to the rainfall-runoff response (Figure 6). End-member variability resulted from replicate sampling at different locations in both tributary catchments (Hooper, 2001) and were considered directly for both approaches and the respective uncertainty estimates (Table 4).

In our direct comparison of EMMA with MixSIAR, we showed that despite the complexity of runoff generation in steep tropical headwaters, the two approaches yielded relatively similar water source contributions, similar to Rothfuss and Javaux (2017). This is an encouraging result that could pave the way for a more extensive use of Bayesian mixing models in future hydrological studies. However, we still report some discrepancies between the two methods. In particular, results at the event scale can be significantly different (e.g. event 2 in Fig 6) and EMMA seemed to perform better than MixSIAR with lower error bars. We postulate that Bayesian approaches are more adapted to larger datasets and less able to represent temporal dynamics with a lower number of samples per event, especially when no prior assumption is included in the model. However, we also recognize that different Bayesian approaches can perform differently. For instance, Beria et al. (2020) found their Bayesian modeling framework to work well with small sample sizes. In contrast, for all samples considered to contribute to the main stream and the tributaries (Figure 5), MixSIAR resulted in a lower overall uncertainty compared to EMMA, as also detected by Rothfuss and Javaux (2017) and He et al. (2020). While He et al. (2020) partly attributed the better performance of their Bayesian approach to the use of prior distributions, our results show that using generalist priors can also yield robust results. Therefore, we believe MixSIAR is a more versatile framework than EMMA when i) a large number of sources are assumed, even with only few measured tracers, and ii) some of the stream tracer data (mixture) fall outside the EMMA-PCA space (e.g. some tributary samples in Figure 4). Nonetheless, the Bayesian approaches have mostly been developed for 2 to 3 stable isotope tracers (Parnell et al., 2013), and when large tracer data sets are available, the EMMA approach can help with tracer selection and end-member definition as per Hooper (2003). We therefore

emphasize the utility of our approach of combining an initial EMMA analysis with a comparison using a Bayesian approach. This method could also be used to inform prior distributions for input to further reduce uncertainties (Ogle et al., 2014).

5. Conclusions

We have shown that in the undisturbed San Lorencito rainforest headwater catchment, runoff is predominantly generated via shallow soil flow pathways (0-15 cm depth). This finding is in line with earlier model hypotheses (Dehaspe et al., 2018) and recent water age estimates of a tracer-aided model (Correa et al., 2020) that could only simulate the rainfall-runoff and isotope response of the stream using fast, near-surface runoff generation algorithms and a younger water dominance. We used a rather short, but spatio-temporally intense field measurement campaign following Riveros-Iregui et al. (2018) in absence of longer-term and continuous data records in the tropics. Despite uncertainties related to assumptions of time and space-invariant end-members, we were able to use multiple conservative tracers (Barthold et al., 2012; Correa et al., 2017; 2018) and two mixing model frameworks (EMMA and MixSIAR) to examine runoff generation and dominant flow pathways in this catchment. We summarize our main findings here:

- EMMA and MixSIAR provided similar water source contributions to the stream mixtures and can be considered complimentary methods that inform each other.
- EMMA is a particularly useful diagnostic tool to select conservative tracers and end-members, while MixSIAR is more efficient in the case of a larger number of sources.

- Additional water age dating with tritium further emphasized the shallow streamflow sources with little evidence for older and deeper water contributions to the stream.
- The application of an ensemble of methods allowed us to study the interaction of shallow flow paths, runoff generation and water source dynamics at the event scale, and to present reliable results based on the consensus of all methodologies.
- Saturation excess surface runoff under the most extreme events and shallow lateral sub-surface runoff together form the dominant near-surface flow pathways.
- The conceptualization of baseflow depends on the method used and does not always describe the same flow pathways.
- Geomorphological differences between the two hillslope tributaries resulted in distinct hydrochemical signatures with a smaller deep soil water contribution from the steeper hillslope.
- Short-term, intense field measurement campaigns provide an excellent opportunity for a deeper understanding of hydrological processes in under-monitored tropical rainforest catchments.

Acknowledgements

The authors would like to thank the helpful staff at the ReBAMB station for support during the extensive fieldwork campaign and the major sampling effort by Katrin Schulz and Julia Balzer. AC acknowledges a UCR-funded postdoctoral research fellowship. CB would like to acknowledge UCR support for the projects B8709, ED-3319 and UCREA-B8276 and the IAEA CRP22009. CD thanks Dr Dioni Cendón and ANSTO for streamwater tritium analyses and the Australian Research

Council for a postdoctoral fellowship. RSM thanks the support of the GNIP-IAEA for monthly and event-based tritium analysis of rainfall.

DATA AVAILABILITY STATEMENT

The data that support the findings of this research are available from the corresponding author upon request.

References

Arnold, J. G., Allen, P. M. 1999. Automated methods for estimating baseflow and ground water recharge from streamflow records. J. Am. Water Resources Assoc. 35 (2), 411–424.

Balzer, L., Schulz, K., Birkel, C., Biester, H. 2020. Iron oxides control sorption and mobilisation of iodine in a tropical rainforest catchment. SOIL Discuss., https://doi.org/10.5194/soil-2020-20, 2020.

Barnes, C.J., Bonell, M. 1996. Application of unit hydrograph techniques to solute transport in catchments. Hydrological Processes. 10, 793-802.

Barthold, F. K., Tyralla, C., Schneider, K., Vaché, K. B., Frede, H.-G., Breuer, L. 2011. How many tracers do we need for end member mixing analysis (EMMA)? A sensitivity analysis. Water Resour. Res. 47(8), W08519, doi:10.1029/2011WR010604.

Barthold, F. K., Woods, R.A. 2015. Stormflow generation: A meta-analysis of field evidence from small, forested catchments. Water Resour. Res. 51, 3730–3753, doi:10.1002/2014WR016221.

Beria, H., Larsen, J.R., Michelon, A., Ceperley, N.C., Schaefli, B. 2020. HydroMix v1.0: a new Bayesian mixing framework for attributing uncertain hydrological sources. Geoscientific Model Development. 13, 2433-2450.

Birkel, C., Soulsby, C., Tetzlaff, D. 2012. Modelling the impacts of land cover change on streamflow dynamics of a tropical rainforest headwater catchment. Hydrological Sciences Journal. DOI: 10.1080/02626667.2012.728707.

Birkel, C., Geris, J., Molina, M.J., Mendez, C., Arce, R., Dick, J., Tetzlaff, D., Soulsby, C. 2016. Hydroclimatic controls on non-stationary stream water ages in humid tropical catchments. Journal of Hydrology. 542, 231-240. DOI: 10.1016/j.jhydrol.2016.09.006.

Birkel, C., Correa-Barahona, A., Martinez-Martinez, M., et al. 2020. Headwaters drive streamflow and lowland tracer export in a large-scale humid tropical catchment. Hydrological Processes. 2020, 1– 18. https://doi.org/10.1002/hyp.13841

Bonell, M., Gilmour, D.A. 1978. The development of overland flow in a tropical rainforest catchment. Journal of Hydrology. 39 (3–4), 365-382, https://doi.org/10.1016/0022-1694(78)90012-4.

Bonell, M., Bruijnzeel, L.A. 2005. Forests, Water and People in the Humid Tropics. Cambridge University Press: Cambridge. DOI: 10.1017/CBO9780511535666.020.

Blake, W.H., Boeckx, P., Stock, B.C. et al. 2018. A deconvolutional Bayesian mixing model approach for river basin sediment source apportionment. Sci Rep 8, 13073 (2018) doi:10.1038/s41598-018-30905-9

Bruijnzeel, L.A. 2004. Hydrological functions of tropical forests: not seeing the soil for the trees? Agriculture, Ecosystems & Environment. 104(1), 185-228, https://doi.org/10.1016/j.agee.2004.01.015.

Bücker, A., Crespo, P., Frede, H.-G., Vaché, K., Cisneros, F. 2010. Identifying Controls on Water Chemistry of Tropical Cloud Forest Catchments: Combining Descriptive Approaches and Multivariate Analysis. Hydrology and Earth System Sciences. 16(1), 127–149, 2010.

Cassells, D.S., Gilmour, D.A., Bonell, M. 1985. Catchment response and watershed management in the tropical rainforests in north-eastern Australia. Forest Ecology and Management**.** 10, 155-175.

Chang, J.H., Lau, L.S. 1983. Definition of the humid tropics. In Hydrology and Water Management in the Humid Tropics, Bonell M, Hufschmidt MM, Gladwell JS (eds.). Cambridge University Press: Cambridge; 571–575.

Chaves, J., Neill, C., Germer, S., Neto, S. G., Krusche, A., Elsenbeer, H. 2008. Land management impacts on runoff sources in small Amazon watersheds. Hydrological Processes, 22, 1766–1775. https://doi.org/10.1002/hyp.6803

Christophersen, N., Neal, C., Hooper, R. P., Vogt, R. D., Andersen, S. 1990. Modelling streamwater chemistry as a mixture of soilwater end-members - A step towards second-generation acidification models. J. Hydrol. 116(1–4), 307–320, 1990.

Clark, K. E., Torres, M. A., West, A. J., Hilton, R. G., New, M., Horwath, A. B., Fisher, J. B., Rapp, J. M., Robles Caceres, A., Malhi, Y. 2014. The hydrological regime of a forested tropical Andean catchment. Hydrol. Earth Syst. Sci. 18, 5377–5397, https://doi.org/10.5194/hess-18-5377-2014.

Correa, A., Windhorst, D., Tetzlaff, D., Crespo, P., Célleri, R., Feyen, J., Breuer, L. 2017. Temporal dynamics in dominant runoff sources and flow paths in the Andean Páramo. Water Resour. Res. 53, 5998–6017, https://doi.org/10.1002/2016WR020187, 2017.

Correa, A., Breuer, L., Crespo, P., Célleri, R., Feyen, J., Birkel, C., Silva, C., Windhorst, D. 2018. Spatially distributed hydro-chemical data with temporally high-resolution is needed to adequately assess the hydrological functioning of headwater catchments. Sci. Total Environ. 651, 1613–1626, https://doi.org/10.1016/j.scitotenv.2018.09.189.

Correa, A., Ochoa-Tocachi, D., Birkel, C. 2019. Technical note: Uncertainty in multi-source partitioning using large tracer data sets. Hydrology and Earth System Sciences. 1–14, doi: https://doi.org/10.5194/hess-2019-197.

Correa, A., Birkel, C., Gutierrez, J., Dehaspe, J., Durán-Quesada, A.M., Soulsby, C., Sánchez-Murillo, R. 2020. Modelling non-stationary water ages in a tropical rainforest: A preliminary spatially distributed assessment. Hydrological Processes. 1– 18. https://doi.org/10.1002/hyp.13925

Davis, P., J. Syme, J. Heikoop, J. Fessenden-Rahn, G. Perkins, B. Newman, A. E. Chrystal, S. B. Hagerty 2015. Quantifying uncertainty in stable isotope mixing models. J. Geophys. Res. Biogeosci. 120, 903–923, doi:10.1002/2014JG002839.

Dehaspe, J., Birkel, C., Tetzlaff, D., Sánchez-Murillo, R., Durán-Quesada, A.M., Soulsby, C. 2018. Spatially distributed tracer-aided modelling to explore water and isotope transport, storage and mixing in a pristine, humid tropical catchment. Hydrological Processes 32, 3206– 3224. https://doi.org/10.1002/hyp.13258.

Denyer, P., Montero, W., Alvarado, G.E. 2003. Atlas tectónico de Costa Rica. UCR: San José.

Duvert, C., Hutley, L. B., Birkel, C., Rudge, M., Munksgaard, N. C., Wynn, J. G., et al. 2020. Seasonal shift from biogenic to geogenic fluvial carbon caused by changing water sources in the wet-dry tropics. Journal of Geophysical Research: Biogeosciences, 125, e2019JG005384. https://doi.org/10.1029/2019JG005384

Elsenbeer, H., Lack, A., Cassel, K. 1995. Chemical fingerprints of hydrological compartments and flow paths at La Cuenca, Western Amazonia. Water Resour. Res. 31 (12), 3051–3058.

Elsenbeer, H. 2001. Hydrologic flowpaths in tropical rainforest soilscapes—a review. Hydrol. Process. 15, 1751–1759.

Fagan, M.E., DeFries, R.S., Sesnie, S.E., Arroyo, J.P., Walker, W., Soto, C., Chazdon, R.L., Sanchun, A. 2013. Land cover dynamics following a deforestation ban in northern Costa Rica. Environmental Research Letters. 8. DOI: 10.1088/1748-9326/8/3/034017.

Farrick, K. K., Branfireun, B. A. 2015. Flowpaths, source water contributions and water residence times in a Mexican tropical dry forest catchment. J Hydrol 529, 854–865.

Genereux, D. P., Webb, M., Solomon, D. K. 2009. Chemical and isotopic signature of old groundwater and magmatic solutes in a Costa Rican rain forest: Evidence from carbon, helium, and chlorine. Water Resour. Res. 45, W08413, doi:10.1029/2008WR007630.

Giorgi, F. 2006. Climate change hot-spots. Geophysical Research Letters. 33. DOI: 10.1029/2006GL025734.

González, J.E., Georgescu, M., Lemos, M.C., Hosannah, N., Niyogi, D. 2017. Climate change's pulse is in Central America and the Caribbean. Eos 98. DOI: 10.1029/2017EO071975.

Gröning, M., Lutz, H. O., Roller-Lutz, Z., Kralik, M., Gourcy, L., Pöltenstein, L. 2012. A simple rain collector preventing water re-evaporation dedicated for δ18O and δ2H analysis of cumulative precipitation samples. Journal of Hydrology, 448-449, 195–200. https:// doi.org/10.1016/j.jhydrol.2012.04.041

He, Z., Unger-Shayesteh, K., Vorogushyn, S., Weise, S.M., Duethmann, D., Kalashnikova, O., Gafurov, A., Merz, B. 2020. Comparing Bayesian and traditional end-member mixing approaches for hydrograph separation in a glacierized basin. Hydrology and Earth System Sciences. 24, 3289-3309.

Holwerda, F., Scatena, F.N., Bruijnzeel, L.A. 2006. Throughfall in a Puerto Rican lower montane rain forest: A comparison of sampling strategies. Journal of Hydrology. 327, 592–602. https://doi.org/10.1016/j.jhydrol.2005.12.014

Hooper, R. P. 2001. Applying the scientific method to small catchment studies: a review of the Panola Mountain experience. Hydrol. Process. 15(10), 2039–2050, doi:10.1002/hyp.255, 2001.

Hooper, R. P. 2003. Diagnostic tools for mixing models of stream water chemistry. Water Resour. Res. 39(3), 1–13, doi:10.1029/2002WR001528, 2003.

James, A. L., Roulet, N. T. 2006. Investigating the applicability of end-member mixing analysis (EMMA) across scale: A study of eight small, nested catchments in a temperate forested watershed. Water Resour. Res. 42, 1–17, doi:10.1029/2005WR004419, 2006.

Johnson, M.S., Lehmann, J., Couto, E.G., Filho, J.P.N., Riha, S.J. 2006. DOC and DIC in flowpaths of Amazonian headwater catchments with hydrological contrasting soils. Biogeochemistry. 81, 45–57. doi:10.1007/s10533-006-9029-3.

Liu, F., Williams, M. W., Caine, N. 2004. Source waters and flow paths in an alpine catchment, Colorado Front Range, United States. Water Resour. Res. 40(9), W09401, doi:10.1029/2004WR003076, 2004.

Loescher, H.W., Powers, J.S., Oberbauer, S.F. 2002. Spatial variation of throughfall volume in an old-growth tropical wet forest, Costa Rica. Journal of Tropical Ecology. 18, 397-407. DOI: 10.1017/S0266467402002274.

Małoszewski P., Zuber A. 1982. Determining the turnover time of groundwater systems with the aid of environmental tracers: 1. Models and their applicability. Journal of Hydrology 57, 207-231.

Moore, I. D., Burch, G. J. 1986. Sediment Transport Capacity of Sheet and Rill Flow: Application of Unit Stream Power Theory. Water Resour. Res. 22(8), 1350– 1360, doi:10.1029/WR022i008p01350.

Monfreda, C., Patz, J.A., Prentice, C., Ramankutty, N., Snyder, P.K. 2005. Global Consequences of Land Use. Science. 309. DOI: 10.1126/science.1111772.

Muñoz-Jiménez R, Giraldo-Osorio JD, Brenes-Torres A, et al. 2018. Spatial and temporal patterns, trends and teleconnection of cumulative rainfall deficits across Central America. Int J Climatol. 1– 14. https://doi.org/10.1002/joc.5925

Muñoz-Villers, L.E., McDonnell, J.J. 2012. Runoff generation in a steep, tropical montane cloud forest catchment on permeable volcanic substrate. Water Resources Research. 48. DOI: 10.1029/2011WR011316.

Nathan, R. J.; McMahon, T. A. 1990. Evaluation of automated techniques for base flow and recession analyses. Water Resour. Res. 26(7), 1465–1473.

Newbold, J. D., Sweeney, B. W., Jackson, J. K., Kaplan, L. A. 1995. Concentrations and export of solutes from six mountain streams in Northwestern Costa Rica. Journal of the North American Benthological Society, 14(1), 21–37. https://doi.org/10.2307/1467722

Ogle, K., Tucker, C., Cable, J. M. 2014. Beyond simple linear mixing models: Process-based isotope partitioning of ecological processes. Ecological Applications, 24(1), 181-195. https://doi.org/10.1890/1051-0761-24.1.181

Parnell A.C., Phillips D.L., Bearhop S., Semmens B.X., Ward E.J., Moore J.W., Jackson A.L., Grey J., Kelly D.J., Inger R. 2013. Bayesian stable isotope mixing models. Environmetrics 24, 387-399.

Phillips, D. L., Gregg, J. W. 2001. Uncertainty in source partitioning using stable isotopes. Oecologia 127(2), 171–179, doi:10.1007/s004420000578, 2001.

Phillips, D.L., Gregg, J.W. 2003. Source partitioning using stable isotopes: coping with too many sources. Oecologia. 136, 261-269.

R Development Core Team. 2019. R: A Language and Environment for Statistical Computing. R Foundation for Statistical Computing: Vienna.

Riley, S. J., S. D. DeGloria, Elliot, R. 1999. A terrain ruggedness index that quantifies topographic heterogeneity. Intermountain Journal of Sciences. 5(1-4).

Riveros-Iregui DA, Covino TP, González-Pinzón R. 2018. The importance of and need for rapid hydrologic assessments in Latin America. Hydrological Processes 32, 2441–2451. https://doi.org/10.1002/hyp.13163

Rothfuss, Y., Javaux, M. 2017. Reviews and syntheses: Isotopic approaches to quantify root water uptake: a review and comparison of methods. Biogeosciences, 14, 2199–2224, https://doi.org/10.5194/bg-14-2199-2017.

Salazar-Rodríguez, A.H. 2003. Reserva Biológica Alberto Manuel Brenes: Una excepción en Costa Rica. Revista InterSedes 8.

Scholl, M.A., J.B. Shanley, S.F. Murphy, J.K. Willenbring, M. Occhi, González, G. 2015. Stable-isotope and solute-chemistry approaches to flow characterization in a forested tropical watershed, Luquillo Mountains, Puerto Rico. Applied Geochemistry 63, 484-497.

Shanley, J.B., McDowell, W.H., Stallard, R.F. 2011. Long-term patterns and short-term dynamics of stream solutes and suspended sediment in a rapidly weathering tropical watershed. Water Resources Research. 47. DOI: 10.1029/2010WR009788.

Sidle, R.C., Ziegler, A.D., Negishi, J.N., Nik, A.R., Siew, R., Turkelboom, F. 2006. Erosion processes in steep terrain – truths, myths, and uncertainties related to forest management in Southeast Asia. Forest Ecol. Manage. 224, 199–225. doi:10.1016/j.foreco.2005.12.019.

Solano-Rivera, V., Geris, J., Granados-Bolaños, S., Brenes-Cambronero, L., Artavia-Rodríguez, G., Sánchez-Murillo, R., Birkel, C. 2019. Exploring extreme rainfall impacts on flow and turbidity dynamics in a steep, pristine and tropical volcanic catchment. Catena, 182, 104118, doi:10.1016/j.catena.2019.104118.

Solomon, D. K., Genereux, D. P., Plummer, L. N., Busenberg, E. 2010. Testing mixing models of old and young groundwater in a tropical lowland rain forest with environmental tracers. Water Res. Research 46, W04518.

Soulsby, C., J. Petry, M. J. Brewer, S. M. Dunn, B. Ott, Malcolm, I.A. 2003. Identifying and assessing uncertainty in hydrological pathways: A novel approach to end member mixing in a Scottish agricultural catchment. J. Hydrol. 274(1-4), 109–128, doi:10.1016/S0022-1694(02)
00398-0.

Stewart M.K., Morgenstern U., McDonnell J.J. 2010. Truncation of stream residence time: how the use of stable isotopes has skewed our concept of streamwater age and origin. Hydrol. Process. 24, 1646–1659, doi:10.1002/hyp.7576.

Stock B.C., Semmens B.X. 2016. MixSIAR GUI User Manual. Version 3.1. https://github.com/brianstock/MixSIAR.

Stock, B.C., Jackson, A.L., Ward, E.J., Parnell, A.C., Phillips, D.L., Semmens, B.X. 2018. Analyzing mixing systems using a new generation of Bayesian tracer mixing models. PeerJ. 6:e5096.

Thomas, MF. 1994. Geomorphology in the Tropics: A Study of Weathering and Denudation in Low Latitudes. John Wiley and Sons: Chichester.

van Meerveld, H. J. I., Zhang, J., Tripoli, R., Bruijnzeel, L. A. 2019. Effects of reforestation of a degraded *Imperata* grassland on dominant flow pathways and streamflow responses in Leyte, the Philippines. Water Resources Research, 55, 4128– 4148. https://doi.org/10.1029/2018WR023896

Walker, C. D., Richardson, S. B. 1991. The use of stable isotopes of water in characterizing the source of water in vegetation. Chem. Geol. 94, 145–158, doi:10.1016/0168-9622(91)90007-J, 1991.

Willmott, C., Matsuura, K. 2001. Terrestrial air temperature and precipitation: monthly and annual time series (1950–1999). Available at: http://climate.geog.udel.edu/~climate/html_pages/README.ghcn_ts2.html (Accessed 1st February 2018).

Wohl, E., Barros, A., Brunsell, N., Chappell, N., Coe, M., Giambelluca, T., Goldsmith, S., Harmon, R., Hendrickx, J., Juvik, J., McDonnell, J., Ogden, F. 2012. The hydrology of the humid tropics. Nature Climate Change. 2, 655-662. DOI: 10.1038/nclimate1556.

Wymore, A. S., Brereton, R. L., Ibarra, D. E., Maher, K., McDowell, W. H. 2017. Critical zone structure controls concentration-discharge relationships and solute generation in forested tropical montane watersheds. Water Resources Research 53, 6279–6295. https://doi.org/ 10.1002/2016WR020016

Zhang, Z., Tao, F., Shi, P., Xu, W., Sun, Y., Fukushima, T., Onda, Y. 2010. Characterizing the flush of stream chemical runoff from forested watersheds. Hydrological Processes 24(20), 2960 - 2970. DOI: 10.1002/hyp.7717.

Chishan Zhang, Lei Ma, Jin Chen, Yuhan Rao, Yuan Zhou, Xuehong Chen 2019. Assessing the impact of endmember variability on linear Spectral Mixture Analysis (LSMA): A theoretical and simulation analysis. Remote Sensing of Environment 235, 111471, https://doi.org/10.1016/j.rse.2019.111471.

Zimmermann, A., Wilcke, W., Elsenbeer, H. 2007. Spatial and temporal patterns of throughfall quantity and quality in a tropical montane forest in Ecuador. Journal of Hydrology 343 (1-2), 80-96.

Zimmermann, A., Germer, S., Neill, C., et al. 2008. Spatio-temporal patterns of throughfall and solute deposition in an open tropical rain forest. Journal of Hydrology 360, 87–102. https://doi.org/10.1016/j.jhydrol.2008.07.028

Zimmermann, A., Francke, T., Elsenbeer, H. 2012. Forests and erosion: Insights from a study of suspended-sediment dynamics in an overland flow-prone rainforest catchment. Journal of Hydrology 27, 170-181. DOI: 10.1016/j.jhydrol.2012.01.039.

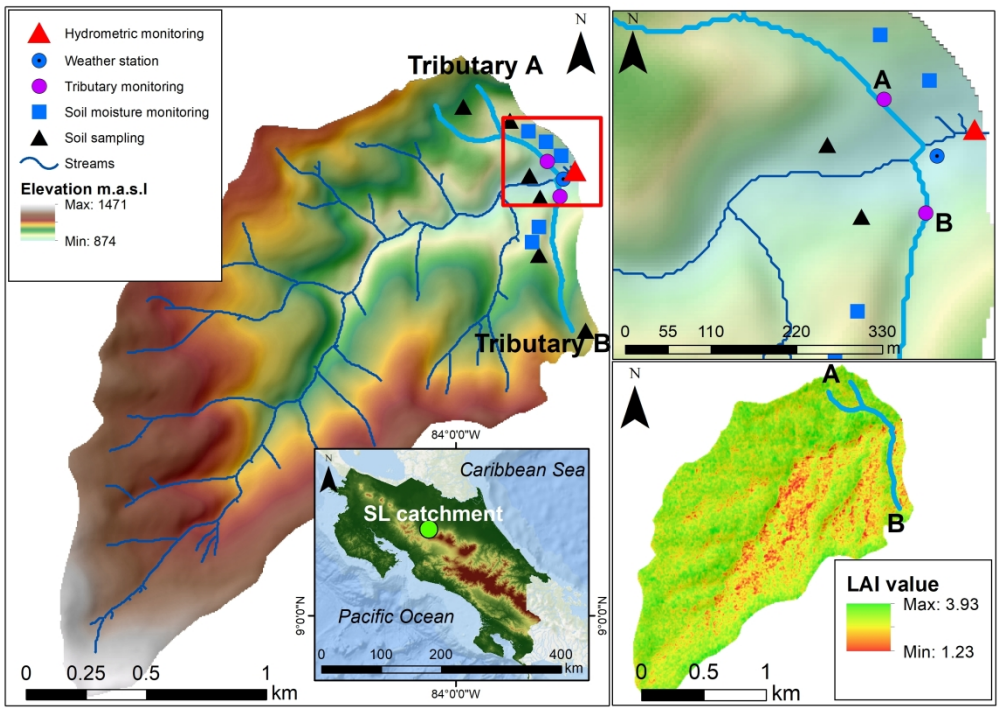

Figure 1: The regional context of the San Lorencito study catchment with monitored sub-catchment tributaries located on hillslopes A and B, automatic weather station in the forest used for this measurement campaign (blue circle), soil moisture (blue rectangles) and sampling (black triangles) locations, topography and a satellite-derived leaf area index (LAI) map (Dehaspe et al., 2018). The catchment outlet hydrometric and chemistry monitoring station is shown with the red triangle.

297x210mm (300 x 300 DPI)

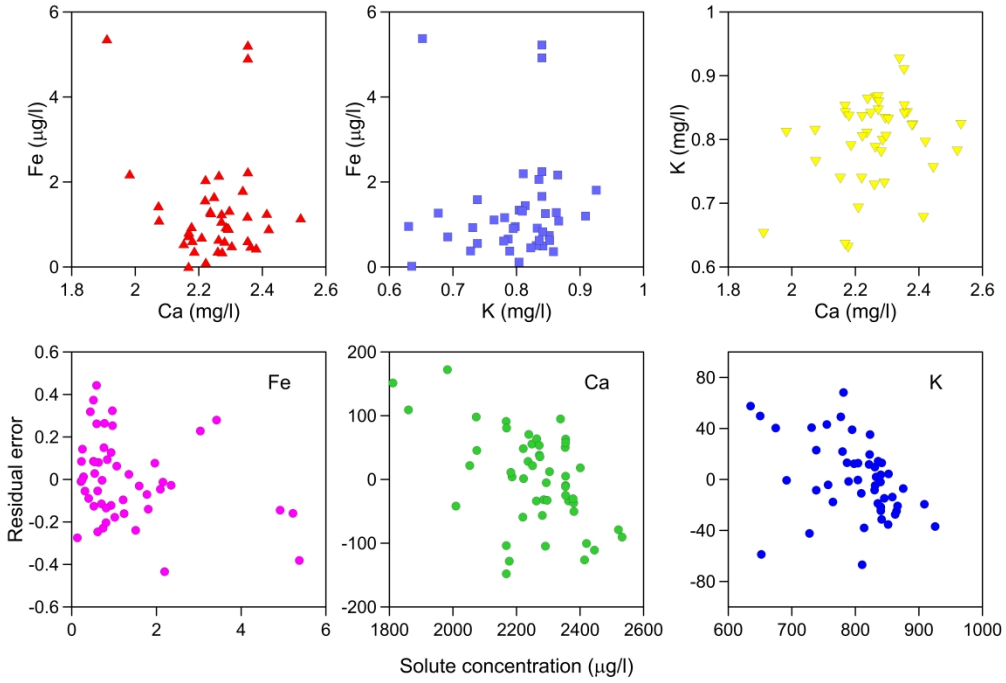

Figure 2: Bi-variate plots (upper row) of conservative tracers and resulting unstructured residual error plots of Fe, Ca and K stream chemical parameters (lower row) aiding selection of conservative tracers without structure in the residuals.

598x403mm (300 x 300 DPI)

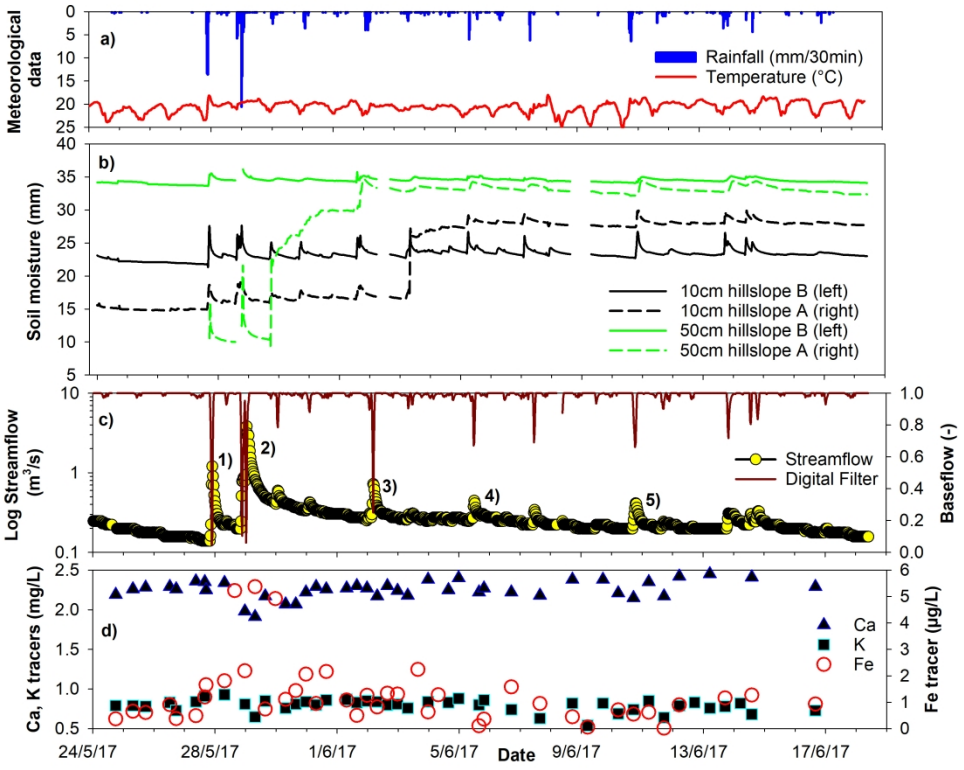

Figure 3: Time series plots of the four-weeks sampling period from 24th May to 18th June 2017 showing a) 30 min throughfall, air temperature, b) averaged soil moisture at 10 cm and 50 cm depth for each sub-catchment on hillslope A and B and c) streamflow at the outlet with a digital filter derived baseflow fraction. The last panel d) shows the three selected tracer (Ca, K, Fe) concentration time series in streamflow at the outlet.

279x215mm (300 x 300 DPI)

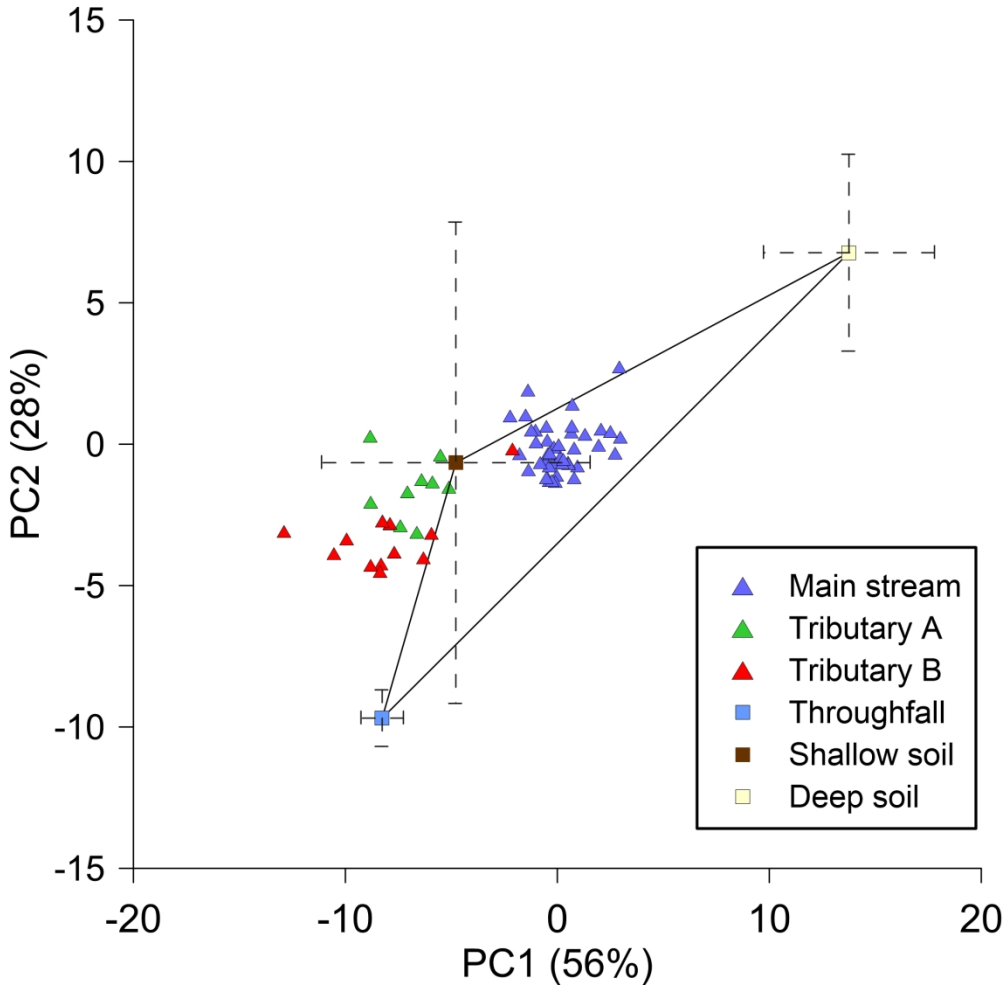

Figure 4: EMMA mixing diagram using ordered Eigenvectors and source water contributions (throughfall, shallow and deep soils) to the main stream and both sub-catchment tributaries A and B, explaining 84% of the total variance. The error bars represent the first standard deviation of measured concentrations. The single composite throughfall sample was assigned a standard deviation of one.

179x176mm (300 x 300 DPI)

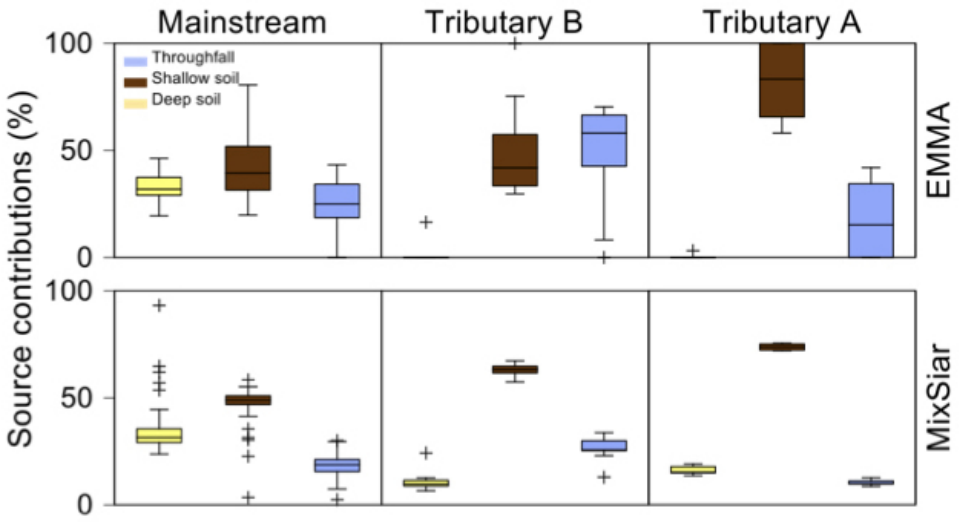

Figure 5: The EMMA (upper panel) and MixSIAR (lower panel) derived source water contributions to the main stream at the outlet, sub-catchment tributary A and B. The boxplots represent the distribution of potential source water contributions derived by a Bayesian approach for MixSIAR and a Taylor series approximation for EMMA. Throughfall (light blue), shallow (brown) and deep (yellow) soil source waters are similarly color coded throughout the paper. The boxes show the median and 25th/75th percentiles with the whiskers indicating the 5th/95th percentiles. The crosses point out absolute extreme values.

230x125mm (72 x 72 DPI)

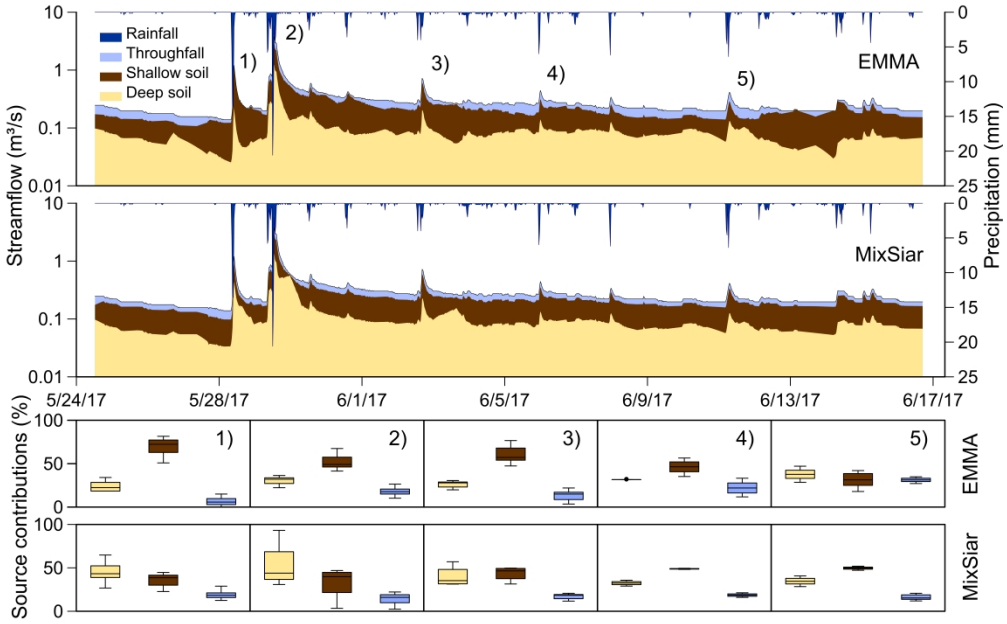

Figure 6: a) EMMA and b) MixSIAR interpolated hydrograph separation time series and source water contributions for each of the five events separately assuming time-invariant end-members (same color code as in previous plots).

584x373mm (300 x 300 DPI)

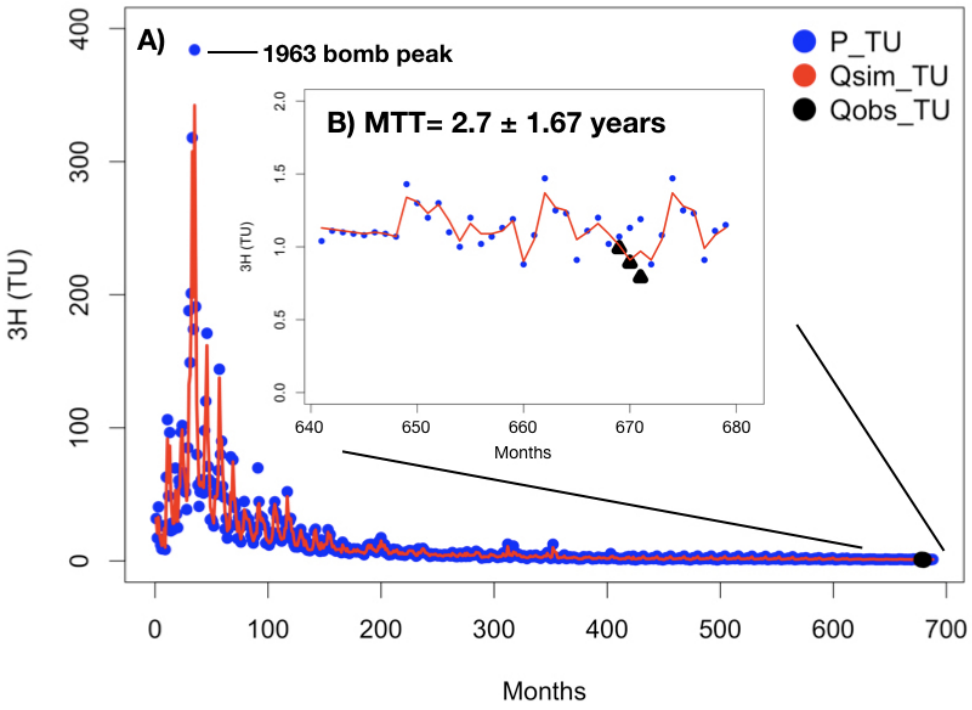

Figure 7: The best-fit tritium-based mean transit time (MTT) estimate of baseflow in the San Lorencito stream (Qsim_TU) using reconstructed long-term monthly precipitation volumes (NCEP re-analysis product) and tritium measurements from nearby IAEA stations (Florida and California) merged with recent rainfall measurements in Costa Rica (P_TU) fitted to match the observed tritium in streamflow at the outlet (Qobs_TU).

289x215mm (72 x 72 DPI)